CHEMISTRY
AN ASIAN JOURNAL
ACES
FULL PAPER

DOI: 10.1002/asia.201402635

Exclusive Detection of Sub-Nanomolar Levels of Palladium(II) in Water: An Excellent Probe for Multiple Applications

Namita Kumari,[a] Nilanjan Dey,[a] Krishan Kumar,[a] and Santanu Bhattacharya*[a, b]

Abstract: A new colorimetric probe has been developed for the detection and estimation of Pd^{II} at sub-nanomolar concentrations. The probe consisted of rhodamine (signaling unit), which was linked with a bis-picolyl moiety (binding site) through a phenyl ring. Pd^{II} induced opening of the spirolactam ring of the probe with the generation of a prominent pink color. The excellent selectivity of the probe towards Pd^{II} over Pd^{0} or Rh^{II} ensured its potential utility for the detection of residual palladium contamination in pharmaceutical drugs and in Pd-catalyzed reactions. The probe showed a "turn-on" (bright yellow) fluorescence upon the addition of Pd^{II}, which made it suitable for the detection of Pd contaminants in mammalian cells.

Keywords: fluorescence · palladium · rhodamine · sensors · water

Introduction

Palladium is one of the most important platinum-group elements (PGEs) because of its unique chemical and physical properties.[1] It is widely used in organic synthesis in catalysts for many cross-coupling reactions, such as the Buchwald–Hartwig, Heck, Sonogashira, and Suzuki–Miyaura reactions.[2] One of its best-known applications is in vehicle-exhaust systems, in which it helps to decrease the emission of deadly gaseous pollutants, such as carbon monoxide, hydrocarbons, and nitrogen oxides.[3] However, its extensive use has resulted in a rapid increase in the concentration of palladium in the environment, which can lead to serious health hazards.[4] Moreover, owing to its greater solubility gradient compared to other PGE ions, Pd^{II} has a higher biological uptake and a higher accumulation propensity in the food chain.[5] It binds with thiol-containing amino acids (cystine, homocysteine, methionine, glutathione, etc.) or proteins (casein, silk fibroin, etc.) because of its high thiophilic nature.[5] Thus, a restriction has been imposed on the maximum dietary intake of palladium of $<15\,\mu g$ per person per day.[6] Even the amount of residual palladium in active pharmaceutical ingredients has been restricted to less than 10 ppm.[7]

Various analytical methods, such as atomic absorption spectroscopy, X-ray fluorescence spectroscopy, and plasma emission spectroscopy, have long been used to detect various ions and analytes, even at sub-micromolar concentrations. However, these methods require extensive sample preparation, expensive instrumentation, and are often not cost-effective and may not be widely accessible. To overcome these difficulties, over the past few years, there has been increasing focus on the design and synthesis of various small-molecule-based probes that can detect Pd by using simple UV/Vis and fluorescence spectrophotometry. In 2007, Koide and co-workers reported the first fluorescein-based Pd probe for the detection of palladium below its permitted level in water.[8a] However, to achieve saturation in the spectroscopic response, 1 h incubation time with employment of high pH was required (borate buffer at pH 10). Subsequently, these authors also developed a library of other probes for the detection of palladium in various samples within significantly lower detection times (about 15 min) at pH 7.[8]

Following this report, considerable recent effort has been made towards the naked eye detection of Pd.[9] The diverse sensing pathways employed by these probes often include Pd^{II} complexation or Pd-catalyzed reactions that modulate their photophysical properties.[10] Three procedures have mainly been exploited for the detection of palladium. The first involves the interaction of Pd^{II} with π-electron-rich functionalities, such as propargyl, allyl, and nitrile groups, of which the hydrolysis of propargyl ethers could be catalyzed by both Pd^{0} and Pd^{II} species, thereby rendering similar optical responses. The second approach is the oxidative insertion of Pd^{0} and the third is the coordination of Pd^{II} through multiple coordination sites. In this instance, rhodamine-based sensors are advantageous as signaling moieties, because they

[a] Dr. N. Kumari,[+] N. Dey,[+] K. Kumar, Prof. Dr. S. Bhattacharya
Department of Organic Chemistry
Indian Institute of Science
Bangalore 560012 1 (India)
Fax: (+91) 080-2360-0529
E-mail: sb@orgchem.iisc.ernet.in

[b] Prof. Dr. S. Bhattacharya
Jawaharlal Nehru Centre of Advanced Scientific Research
Bangalore 560012 (India)

[+] These authors contributed equally to this work.

Supporting information for this article is available on the WWW under http://dx.doi.org/10.1002/asia.201402635.

typically exhibit a "turn-on" response. Moreover, their facile synthesis and highly sensitive photophysical properties contribute to their frequent application.[10] However, most of the reported rhodamine-based sensors pose serious drawbacks, including prolonged incubation time, responses only in organic or organic/water mixtures, potential interference with other PGE ions, and no discrimination between Pd^{II} and Pd^{0}.

Considering these practical challenges in the detection of palladium, we have designed a new probe for the efficient sensing of Pd^{II}. This probe shows selective detection of Pd^{II} in water, as well as at physiological pH 7.4, with a "turn-on" signal in both UV/Vis and fluorescence spectroscopy. Moreover, this probe can be used multiple times for the detection of Pd^{II} ions. The real-time application of the probe has been examined by determining residual Pd^{II} in Pd-catalyzed reactions, pharmaceutical products, real-life water samples, and also in glassware that was used for Pd-catalyzed reactions following washing. This probe also showed excellent selectivity for Pd^{II} over Pd^{0}, a property rarely manifested by other probes. Suitable portable test strips have been prepared by using filter paper to check the fast-track detection of Pd ions. Furthermore, the probe was also found to be efficient in detecting Pd^{II} contaminants in mammalian cells.

Results and Discussion

Synthesis

Following our interest in designing small-molecule-based probes,[11] herein we report the synthesis of a new rhodamine derivative (**1**), as shown in Scheme 1 (for details, see the Experimental Section). The structure of the probe was characterized by ^{1}H and ^{13}C NMR spectroscopy and by HRMS (see the Supporting Information).

Absorption and Emission Spectroscopic Studies

A solution of compound **1** in water was both colorless and non-fluorescent, thus indicating the presence of a closed spirolactam ring structure of the probe. The addition of Pd^{II} to the solution resulted in a visible color change from colorless to bright pink (Figure 1, inset). This color change was further monitored by UV/Vis absorption spectroscopy, as shown in Figure 1. The addition of Pd^{II} to an aqueous solution of the probe (10 μM) resulted in an approximate 55-fold increase in the absorbance at 533 nm. The selectivity of the probe towards Pd^{II} was also investigated. The absorbance spectra were recorded upon the addition of various other cations to the probe solution (Figure 1b). The observed changes in absorbance upon the addition of other cations were negligible compared to that with Pd^{II}. Further interference was studied in the presence of excess amounts of other cations. The probe showed a similar increase in absorbance owing to Pd^{II}, even in the presence of excess amounts of other cations (see the Supporting Information, Figure S1). Thus, this probe showed excellent selectivity towards Pd^{II} ions.

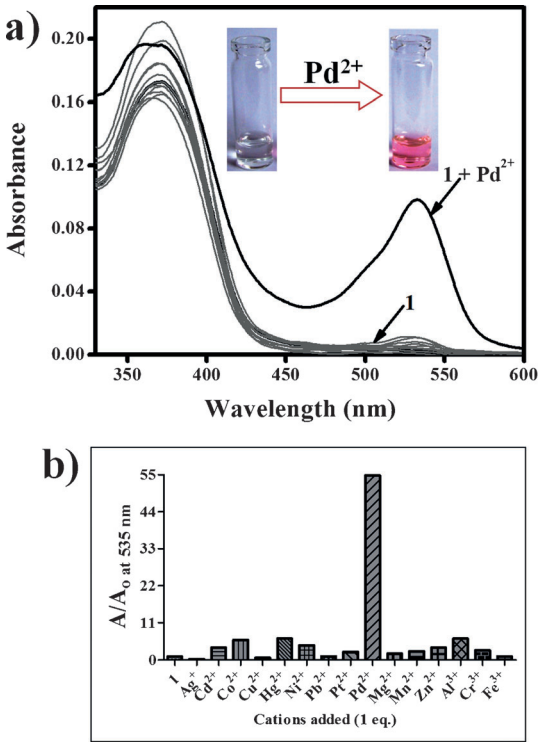

Figure 1. a) Changes in the UV/Vis spectra of compound **1** (10 μM) in water (pH 7.4) upon the addition of various cations (1 equiv; Ag^{+}, Cd^{2+}, Co^{2+}, Cu^{2+}, Hg^{2+}, Ni^{2+}, Pb^{2+}, Mg^{2+}, Mn^{2+}, Zn^{2+}, Al^{3+}, Cr^{3+}, Fe^{3+}, Pt^{2+}, and Pd^{2+}). Inset shows the color change of compound **1** upon the addition of Pd^{2+}. b) Normalized absorbance of compound **1** (10 μM) at 533 nm upon the addition of various cations.

UV/Vis titration of compound **1** was performed with the gradual addition of Pd^{II} (see the Supporting Information, Figure S2). Saturation in absorbance was observed upon

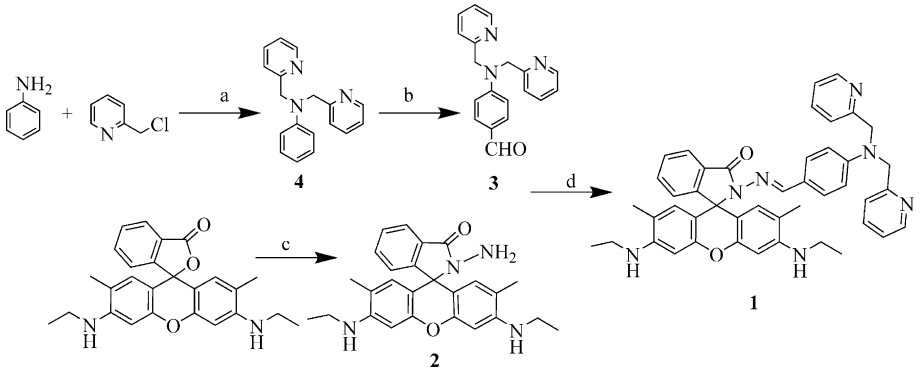

Scheme 1. Synthesis of compound **1**: a) K_2HPO_4/MeCN , reflux, 24 h; b) $POCl_3$/DMF, 90 °C, 2 h; c) NH_2–NH_2/MeOH, reflux, 2 h; d) MeOH, AcOH (cat.), RT, 4 h.

the addition of only 1 equivalent of Pd^{II} (see the Supporting Information, Figure S2b). The stoichiometry of the interaction was determined from a Job plot analysis, which showed a 1:1 interaction between the probe and the Pd^{II} ions, as expected (see the Supporting Information, Figure S3a). The respective binding constant was calculated by using the Benesi–Hildebrand equation for 1:1 stoichiometry. Probe **1** showed a good binding affinity toward Pd^{II} ions, with a binding constant of $\log K = 4.73(\pm 0.01)$ (see the Supporting Information, Figure S3b).

The spectroscopic properties of rhodamine-based sensors are known to be influenced by the pH value of the medium.[12] Thus, we investigated the effect of pH on the sensing process. Pd^{II} was added to solutions of compound **1** at different pH values and the corresponding absorption spectra were recorded. Compound **1** showed the efficient detection of Pd^{2+} above pH 4 (see the Supporting Information, Figure S4) and changes were even observed in the absorption spectra upon the addition of Pd^{II} up to pH 9. Thus, the probe could effectively detect Pd^{II} over a broad pH range (pH 4.5–9).

We further investigated the emission properties of the probe upon the addition of various cations. The solution of compound **1** on its own was non-fluorescent. However, the addition of Pd^{II} ions to the solution resulted in the instantaneous generation of a bright-yellow emission (Figure 2, inset). The emission spectra showed an approximate 10-fold increase in emission intensity upon the addition of Pd^{II} (Figure 2). None of the other cations induced any change in the emission intensity of the probe under identical conditions.

The fluorescence titration experiments were performed with the gradual addition of Pd^{II} ions to the solution of probe **1** (see the Supporting Information, Figure S5). Saturation was observed upon the addition of only 1 equivalent of metal ions. The minimum detectable concentration of Pd^{II} by the probe was 0.59 nM (see the Supporting Information, Figures S6–S8), much lower than the permitted level of Pd^{2+} in drinking water.[8]

The mechanism of fluorescence enhancement upon binding with Pd^{II} was investigated by performing time-dependent emission decay measurements (TCSPC). The fluorescence decay of compound **1** was fitted to a tri-exponential function with time constants of 0.89 (97.5%), 1.64 (2.4%), and 0.27 ns (0.1%). However, upon binding with Pd^{II}, probe **1** only showed a single-exponential decay profile, with a time constant of 0.78 ns (see the Supporting Information, Figure S9). The shorter average decay time in the metal complex (0.78 ns) compared to in the free molecule (0.92 ns) was correlated with opening of the spirolactam ring. Tight binding of the probe to Pd^{II} (higher binding constant) converted the "free-hanging" rhodamine moiety into part of the extended electronic conjugation. In turn, this change resulted in an increase in the number of non-radiative decay channels and a shortening of the average lifetime.[13] The quantum yields were calculated for both the probe and the metal complex; probe **1** showed a quantum yield of 0.05, whereas the metal complex showed a quantum yield of 0.24.

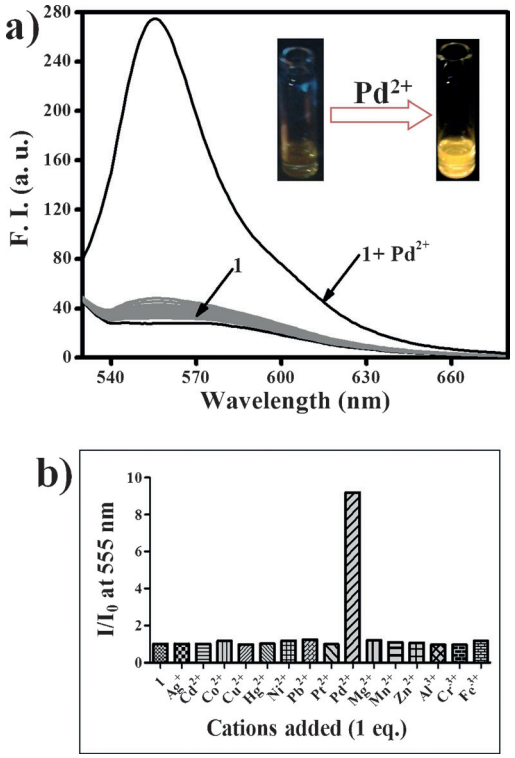

Figure 2. a) Changes in the fluorescence spectra of compound **1** (1 μM, $\lambda_{ex} = 520$ nm) in water (pH 7.4) upon the addition of various cations (1 equiv; Ag^{+}, Cd^{2+}, Co^{2+}, Cu^{2+}, Hg^{2+}, Ni^{2+}, Pb^{2+}, Mg^{2+}, Mn^{2+}, Zn^{2+}, Al^{3+}, Cr^{3+}, Fe^{3+}, Pt^{2+}, and Pd^{2+}). Inset shows the change in fluorescence of compound **1** upon the addition of Pd^{2+} under the irradiation of a UV lamp (365 nm). b) Corresponding normalized emission intensity ratio of compound **1** (1 μM) at 555 nm upon the addition of various cations.

Furthermore, the reversibility of formation of the **1**/Pd^{II} complex was investigated by the addition of ethylenediaminetetraacetic acid (EDTA). The addition of EDTA resulted in the complete recovery of the molecular fluorescence (see the Supporting Information, Figure S10). This result indicated that the probe may be used multiple times for the detection of Pd^{II} ions. Notably, most of the previously reported Pd^{II} sensors suffered from poor discrimination ability between Pd^{II} and Pd^{0}. Therefore, it was important to examine the effect of Pd^{0} on the optical response of the probe. The addition of Pd^{0} induced a very small change in both the absorption and emission spectra, which were negligible compared with the changes on the addition of Pd^{II} (see the Supporting Information, Figure S11). This result confirmed the excellent selectivity of the probe towards Pd^{II} ions over Pd^{0}. Furthermore, the effect of various counteranions was also investigated by using solutions of $PdCl_2$, $Pd(OAc)_2$, and $[Pd(PPh_3)_2Cl_2]$. The individual addition of each salt solution to the probe solution resulted in similar increases in the absorption and emission intensities of compound **1** (see the Supporting Information, Figure S11). This result indicated that the binding process of Pd^{II} with the probe occurred independently of the counteranion.

Mechanism of Detection

The recovery of the molecular signal upon the addition of EDTA supported the reversible ring-opening mechanism of the spirolactam, rather than an ion-catalyzed hydrolysis mechanism. Furthermore, the MS (ESI) spectrum of **1**+Pd^{2+} complex showed a prominent peak at $m/z = 854.2$ $[L(Pd)Cl]^+$ with appropriate isotopic distributions, thereby ensuring 1:1 complexation of the probe to the metal ion (see the Supporting Information, Figure S12). The IR spectra of both the probe and the **1**+Pd^{2+} complex were recorded in water. No significant changes were observed in the frequency of the carbonyl stretch (1650 cm^{-1}; see the Supporting Information, Figure S13), thus indicating the non-involvement of the carbonyl group in the complexation of the probe with palladium ions.

Furthermore, a ^1H NMR spectrum of the probe was also recorded in the presence of Pd^{II} in D_2O/[D_6]DMSO. Significant downfield shifts were observed for the signals of protons H_a, H_d, and H_e, which clearly suggested the involvement of the picolyl nitrogen atoms in the coordination with Pd^{II} (Figure 3). Furthermore, the disappearance of proton H_f confirmed the involvement of the picolyl moiety in the interaction of the probe with Pd^{II}.

The involvement of the picolyl nitrogen atoms was further probed by synthesizing a control molecule that contained a phenyl ring instead of a bis-picolyl unit (see the Supporting Information, Figure S14). This molecule did not show any change upon the addition of Pd^{II} ions, which indicated the significance of the bis-picolyl unit in the binding with the Pd^{II} ions. Thus, we concluded that the probe interacted with the palladium atom through its picolyl unit, which in turn results into opening of the spirolactam ring.[10n]

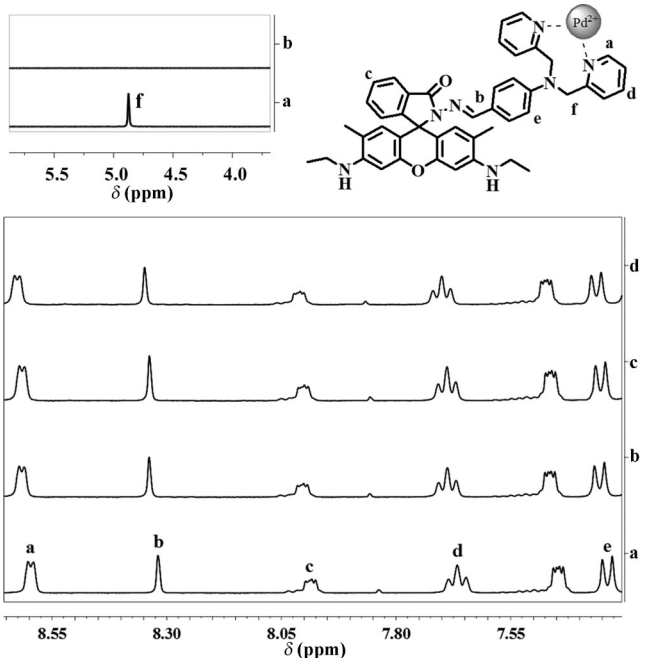

Figure 3. ^1H NMR spectra of compound **1** (10 mM in [D_6]DMSO) after the addition of Pd^{2+} a) 0, b) 0.25, c) 0.5, and d) 1 equiv. Inset shows the molecular structure of probe **1** and partial ^1H NMR spectra of probe **1** before and after the addition of Pd^{II} (1 equiv).

To rationalize the mode of interaction with Pd^{2+}, density functional theory (DFT)-based computational studies were performed at the B3LYP level of theory with the 6-31G* basis set for C, H, and N atoms and the LANL2DZ basis set for Pd atoms. The optimized structures showed close proximity of the aniline nitrogen ($d_{Pd-N1} = 2.11$ Å) and picolyl nitrogen atoms ($d_{Pd-N2} = 2.039$ Å, $d_{Pd-N3} = 2.04$ Å) to the Pd center (Figure 4). The N1–Pd–N2 bond angle was about

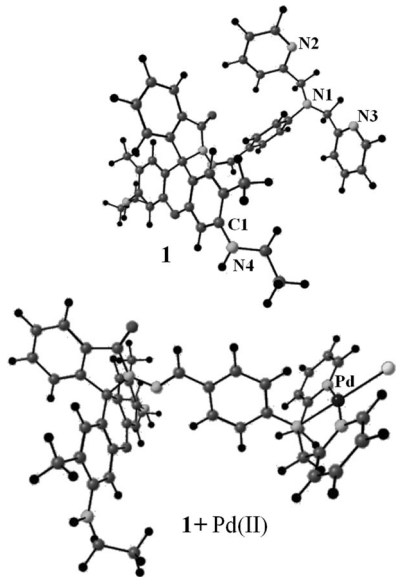

Figure 4. DFT-optimized structures of probe **1** and the **1**/Pd^{2+} complex, as calculated by using the B3LYP/6-31G* basis set for probe **1** and the B3LYP/LANL2DZ basis set for the **1**/Pd^{2+} complex.

96°, thus indicating the formation of a square-planar complex with Pd^{2+}. The effect of electronic push in opening of the spirolactam ring was ascertained from variation in the N4–C1 distance in the isolated probe and its metal (Pd^{2+}) complex. Shortening of the N4–C1 bond length (1.47 Å to 1.39 Å) upon complexation with palladium suggested significant enhancement in the extent of π bonding.

The presence of an orthogonal spirolactam ring in free probe **1** prevented electronic "mixing" of the signaling (xanthene) and recognition units (bis-picolyl). In the free probe, the HOMO was concentrated on the electron-rich xanthene moiety, whereas the LUMO was mainly situated on the bis-picolyl fragment. The addition of Pd^{2+} induced opening of the spirolactam ring and increased the effective conjugation. Furthermore, the HOMO–LUMO band-gap was significantly lower in the metal complex (1.67 eV) than in the free probe (4.14 eV, Figure 5). This lowering of the band-gap was also supported by the experimentally observed bathochromic shift in the UV/Vis spectra of probe **1** upon the addition of Pd^{II}.

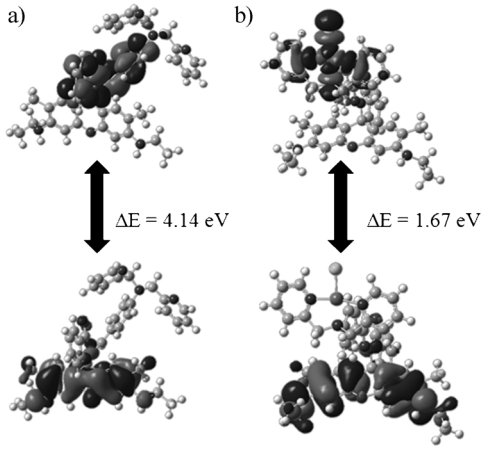

Figure 5. Energy diagrams of the HOMO and LUMO of a) probe **1** and b) the formation of the **1**/Pd^{2+} complex, as calculated by using the B3LYP/6-31G* basis set for probe **1** and the B3LYP/LANL2DZ basis set for the **1**/Pd^{2+} complex.

Various Applications of the Probe

The unique properties of palladium among the PGEs lead to its versatile application in diverse industrial processes, ranging from catalytic converters in the automobile industry to cross-coupling reactions in pharmaceutical drug design. Thus, monitoring of the palladium level in different environmental samples, industrial waste, or pharmaceutical residues is essential to decrease its further accumulation in the biological food chain. To this end, efficient colorimetric sensors may be more useful than other sophisticated techniques, owing to their cost-effectiveness and ease of handling.

The higher solubility gradient of Pd compared to other closely associated PGEs (such as Rh and Pt) is the reason for the increased contamination of Pd^{2+} in drinking water near industrial areas. Therefore, the estimation of Pd levels (must be $<100\ ng\,g^{-1}$) in different natural water sources is crucial to ensuring quality control. For this purpose, we collected water from two commonly used water sources, a city water supply tap and a nearby pool. Then, a known amount of Pd^{II} ions (higher than the permitted level) was added externally to each of these samples. The change in absorbance upon the addition of the probe was recorded immediately in both cases. Linear fits were obtained when changes in the absorbance at 535 nm were plotted against the concentration of added Pd^{II} ions (0.75–3.75 μM), with a correlation coefficient of >0.99, which confirmed that this sensor could be used for the detection of Pd^{II}, even in unknown samples (see the Supporting Information, Figure S15). Then, we compared the estimated concentration of Pd^{II} from the changes in the absorption spectra against the actual amount added. A linear response in both cases suggests that the probe may be able to estimate Pd^{II} concentration without any interference (see the Supporting Information, Figures S16 and S17). The minimum detectable concentrations of Pd^{II} by the probe were approximately 60 nM (tap water) and 63 nM (pool water).[14] All of these observations clearly indicated that probe **1** could effectively estimate the concentration of Pd^{II} ions in real-life water samples.

Then, we investigated whether the probe could detect residual palladium present in glassware in which a reaction had been carried out using a Pd^{II} reagent after normal laboratory washing. A visual color change would help to identify the presence of trace amounts of Pd^{2+} in reusable glassware. Thus, $PdCl_2$ (2 mg) was stirred in THF for 1 h in four different round-bottomed flasks. Then, each flask was washed in various ways (see the Experimental Section). After washing, the probe solution was poured into each of the washed flasks and the optical spectra were recorded (see the Supporting Information, Figure S18). The experiments showed that washing with a laboratory detergent (labolin) or water was not sufficient to completely remove the residual Pd^{II} from the glassware. However, washing with acetone was able to remove most of the residual palladium ions, owing to the higher solubility of Pd^{II} in acetone.

Palladium-catalyzed cross-coupling reactions are widely used in the pharmaceutical industry for drug discovery.[15] Therefore, these drugs are often contaminated with trace amounts of palladium. Herein, the application of the probe was further explored in the determination of the level of contamination of palladium ions in the end products. For this investigation, aspirin was chosen as model drug and a known amount of Pd^{2+} was added externally (for details, see the Experimental Section). When the probe solution was added to this mixture, a visible color change was observed. The extent of spectroscopic change was similar to that with the positive control sample (i.e., with the metal ion alone), which demonstrated the robustness of this probe, even in heterogeneous media (see the Supporting Information, Figure S19).

Owing to the lethal effects of palladium, various governments have imposed restrictions on the allowable level of residual Pd in the end products of Pd-mediated C–C cross-coupling reactions (5–100 ppm). Therefore, it is important to monitor the amount of palladium present in the end reaction mixture. To address this problem, we chose the well-known Suzuki coupling reaction, because it used $Pd(OAc)_2$ as a catalyst. Emission spectra were recorded for the reaction mixture, as well as after standard work-up (for details, see the Experimental Section). The Pd^{II} concentrations before and after work-up were determined by using a calibration curve (as obtained from the titration studies). After work-up, the residual Pd^{II} content was significantly lower than the initial value, although the result was not quantitative because some of the Pd^{2+} had been reduced into Pd^0 during the reaction.

In addition to these results, to obtain an "in-situ" estimation of heavy-metal-ion contamination, we developed portable paper strips. These filter-paper strips were initially soaked in a solution of the probe and dried in air. After that, they were dipped in solutions with different concentrations of Pd^{2+} ions (0.5 and 1 equiv) and a distinct color change with bright-yellow emission was immediately observed (Figure 6).

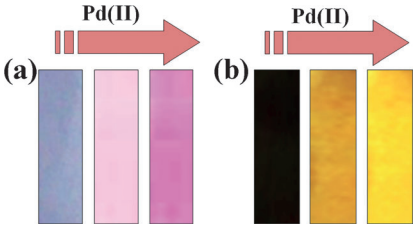

Figure 6. Photographs of test strips of probe **1** (1 mM) for the detection of Pd^{2+} in water: a) in daylight and b) under a UV lamp (365 nm) upon soaking in 0, 0.5, and 1 mM solutions of Pd^{2+} (from left to right).

The application of probe **1** for imaging intracellular Pd^{2+} ions was also investigated by using confocal microscopy. The experiments were performed on a cancer cell line (HeLa cells, Figure 7). First, the cells were incubated with Pd^{2+}

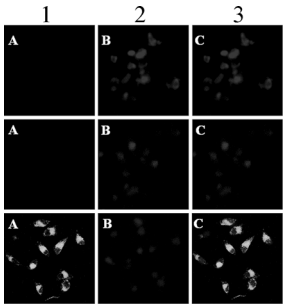

Figure 7. Confocal microscopy images of HeLa cells with the probe. Panel 1: cells incubated with probe **1** alone; panel 2: cells incubated with Pd^{2+} alone; panel 3: cells incubated with both the probe and Pd^{2+}. Confocal microscopy images from the A) yellow and B) blue channels (staining with DAPI) and C) an overlay of images (A) and (B).

(1 μM) for 2 h. Then, they were treated with a solution of compound **1** (10 μM) and incubated for a further 4 h. Control experiments were performed with the metal ion alone and with the probe alone, which were incubated with cells for the same period of time as mentioned above. After processing (see the Supporting Information), the samples were examined under a confocal microscope. The images showed no fluorescence for the cells that were incubated with the probe alone. However, bright-yellow fluorescence was observed for the cells that were incubated in the presence of Pd^{2+} ions. Therefore, this probe may also be useful for the detection of cellular Pd^{2+} contaminants.

Conclusion

In summary, we have developed a new rhodamine-based probe that contained a bis-picolyl binding unit for the effective sub-nanomolar detection of Pd^{II} in water at physiological pH value. The instantaneous "turn-on" response of the probe—both in terms of color and fluorescence emission—upon the addition of Pd^{II} was found to be due to reversible opening of the spirolactam ring. The exact mode of metal-ion coordination was further investigated by ^1H NMR spectroscopy, mass spectrometry, and theoretical investigations. The excellent selectivity of the probe towards Pd^{II} over other closely associated metal ions, such as Pt^{II}, Pd^0, and Rh^{II}, ensured its high potential for versatile real-life applications. The probe could be used as an indicator for Pd^{2+} ions in real water samples. Further applications of the sensor have been demonstrated for the detection of residual palladium contaminants in pharmaceutical drugs or in certain palladium-catalyzed cross-coupling reactions. The "turn-on" response of the probe was also employed for examining Pd^{II}-ion contaminants in cellular samples, thus also indicating its potential for in vivo applications.

Experimental Section

Materials

All of the solvents and reagents were purified and dried by using usual methods. All of the starting materials were obtained from well-known commercial suppliers and used as received. A stock solution of compound (**1**) was made in DMSO and the final concentration of DMSO for all the studies was about 0.1%.

Typical Sensing Procedure

Sensing of the different metal ions in water was performed by adding a solution of probe **1** in DMSO (5 μL/1 μL) to pure water to a final volume of 1 mL ($[\mathbf{1}]=10\times10^{-6}$ M for the UV/Vis experiments, $[\mathbf{1}]=1\times10^{-6}$ M for the fluorescence experiments), followed by the addition of a solution of the metal ions in water (Ag^+, Cd^{2+}, Co^{2+}, Cu^{2+}, Hg^{2+}, Ni^{2+}, Pb^{2+}, Mg^{2+}, Mn^{2+}, Zn^{2+}, Al^{3+}, Cr^{3+}, and Fe^{3+}). The solutions of $PdCl_2$, $[Pd(PPh_3)_2Cl_2]$, $Pd(OAc)_2$, and $PtCl_2$ were prepared according to literature procedures.[16] The effect of pH value on the sensing process was studied by using different buffer solutions with various pH values (HCO_2Na/HCl buffer for pH 2–4.5, CH_3CO_2Na/HCl buffer for pH 5–6.5, Tris/HCl for pH 7–9, $Na_2B_4O_7{\cdot}10H_2O$/NaOH for pH 10–12). All of the studies at pH 7.4 were performed in tris buffer (10 mM).

Instrumentation

^1H and ^{13}C NMR spectra were recorded on a 400 MHz/100 MHz Bruker Advance DRX 400 spectrometer. HRMS analysis was performed on a Q-TOF YA263 high-resolution spectrometer. IR spectra were recorded on a PerkinElmer FTIR spectrometer BX. UV/Vis absorption spectra were recorded on a Shimadzu UV-2100 spectrophotometer. Fluorescence spectra were recorded on a Cary-Eclipse spectrofluorophotometer. The slit-widths for the fluorescence experiments were kept at 5 nm (excitation) and 5 nm (emission) and the excitation wavelength was set at 520 nm for all of the fluorescence experiments.

Sample Preparation for Various Applications

1) Estimation of residual Pd^{II} in laboratory glassware: A solution of $PdCl_2$ (2 mg) in THF (10 mL) was added to four different round-bottomed flasks and the solution was stirred at RT for 1 h. Then, the solution was removed from each flask and the palladium content were determined: 1) in a flask that hadn't been washed and in flasks that were 2) washed with water; 3) brushed with detergent (labolin), followed by washing with water; and 4) brushed with detergent, followed by washing with water and acetone. Then, water (5 mL) was added into all of the flasks. After that, probe **1** was added to each flask ($[\mathbf{1}]=5.0$ μM for the UV/Vis studies, $[\mathbf{1}]=1$ μM for the fluorescence studies) and their corresponding spectra were immediately recorded.

2) Estimation of Pd^{2+} contamination in pharmaceutical drugs: Aspirin (500 mg) was dissolved in MeOH by stirring overnight. Then, the solu-

tion was filtered and, after filtration, the solvent was evaporated. The residue was dissolved in water (50 mL) to prepare a stock solution (10 mg mL^{-1}), to which $PdCl_2$ (5 μM) was added. Then, probe **1** was added and the changes were monitored by UV/Vis and fluorescence spectroscopy (see the Experimental Section).

3) Estimation of Pd^{2+} in the reaction end products: To detect the amount of residual Pd^{II} in a reaction mixture, a Suzuki coupling reaction was performed.[17] $Pd(OAc)_2$ was used in this reaction as a pre-catalyst with a non-nucleophilic carbonate base. Thus, a mixture of 4-bromoanisole (0.5 mmol), phenylboronic acid (0.75 mmol), $Pd(OAc)_2$ (0.25 mol%), K_2CO_3 (1.0 mmol), and water (1.0 mL) was stirred at 100 °C under a N_2 atmosphere for 1 h. Then, the reaction mixture was added to brine (10 mL) and extracted with EtOAc (3×10 mL). The organic solvent was concentrated under vacuum to afford the desired product (18% yield). An aliquot was taken directly from the reaction mixture and probe **1** was added to it. Similarly, an aliquot was removed after work-up of the reaction. During the reaction, most of the Pd^{2+} was converted into Pd^0 and, upon quenching, the remaining active catalyst precipitated as palladium black.[18] This palladium species became insoluble and, therefore, was undetectable by this procedure in the presence of probe **1**.

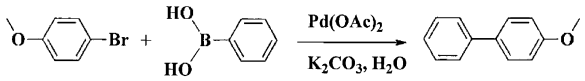

Fluorescence Decay Experiments

Fluorescence lifetime values were measured by using a time-correlated single-photon-counting (TCSPC) fluorimeter (Horiba Jobin Yvon). The system was excited with a 400 nm nano-LED with a pulse duration of 1.2 ns (slit width: 2/2, λ_{em} = 560 nm). The average fluorescence lifetimes (τ_{av}) for the exponential iterative fitting were calculated from the decay times (τ_i) and the relative amplitudes (a_i) by using Equation (1), where a_{1-3} are the relative amplitudes and τ_{1-3} are the lifetime values.

$$\tau_{av} = (a_1\tau_1^2+a_2\tau_2^2+a_3\tau_3^2)/(a_1\tau_1+a_2\tau_2+a_3\tau_3) \quad (1)$$

^{1}H NMR Titration Studies

^{1}H NMR titration experiments were performed for compound **1** (8 mM) in a [D_6]DMSO/D_2O (9:1) mixture with Pd^{2+} (in CD_3OD/D_2O, 1:3, with NaCl). All of the spectra were recorded under identical conditions.

Synthesis

4-[Bis(2-pyridylmethyl)amino] benzaldehyde (**3**):[19] Aniline (0.931 g, 10.0 mmol) and K_2HPO_4 (5.22 g, 30.0 mmol) were dissolved in MeCN (10 mL) and 2-picolyl chloride hydrochloride (4.59 g, 28.0 mmol) was added dropwise at 0 °C and stirred at RT for 30 min. Then, the reaction mixture was heated at reflux for 24 h. Water (a few mL) was added and the reaction mixture was extracted with EtOAc. The intermediate was purified by column chromatography on silica gel. Yield: 92%; brown crystalline solid; ^{1}H NMR (300 MHz, $CDCl_3$): δ = 4.81 (s, 4H), 6.69 (t, J = 8.2 Hz, 3H), 7.14 (t, J = 6.3 Hz, 4H), 7.25 (d, J = 6.9 Hz, 2H), 7.60 (t, J = 7.65 Hz, 2H), 8.57 ppm (d, J = 4.5 Hz, 2H); ^{13}C NMR(75 MHz, $CDCl_3$): δ = 57.2, 112.4, 117.1, 120.7, 121.9, 129.2, 136.8, 148.1, 149.6, 158.8 ppm, IR (neat): $\tilde{\nu}$ = 3062.4, 1590.9, 1506.1, 1434.7, 1351.8, 1047.1, 750.1 cm^{-1}; HRMS: m/z calcd for $C_{18}H_{18}N_3$: 276.150 $[M+H]^+$; found: 276.148.

The intermediate was formylated by adding DMF (5.6 mL, 72.4 mmol) and $POCl_3$ (3.54 g, 23.0 mmol) and stirring at RT for 30 min, followed by heating at 90 °C for 2 h. After completion of the reaction, the mixture was allowed to cool to RT, ice water was added, and the solution was neutralized to pH 7 by adding solid sodium acetate. Then, the mixture was extracted with EtOAc, washed with water, and dried, followed by purification by column chromatography on silica gel. Yield: 92%; ^{1}H NMR (300 MHz, $CDCl_3$): δ = 4.83 (s, 4H), 6.80 (d, J = 9.0 Hz, 2H), 7.22–7.28 (m, 4H), 7.65–7.71 (m, 4H), 8.63 (d, J = 3.9 Hz, 2H), 9.74 ppm (s, 1H); ^{13}C NMR (75 MHz, $CDCl_3$): δ = 56.9, 111.9, 120.6, 122.4, 126.4, 132.0, 137.1, 149.8, 153.0, 157.1 ppm; IR (neat): $\tilde{\nu}$ = 2735.3, 1670.2, 1598.5, 1523.4, 1396.9, 1227.7, 1169.2, 817.3, 750.0 cm^{-1}; MS(ESI): m/z: 326 $[M+Na]^+$; HRMS: m/z calcd for $C_{19}H_{17}N_3ONa$: 326.1269 $[M+Na]^+$; found: 326.1266.

Rhodamine hydrazone (**2**): Rhodamine-6G hydrazone (**4**) was prepared according to a literature procedure.[12,20] Briefly, in a 50 mL round-bottomed flask, rhodamine-6G (**5**, 0.479 g, 1 mmol) was dissolved in EtOH (15 mL). To that, excess hydrazine monohydrate (85%, 1.5 mL) was added dropwise with vigorous stirring at RT. Then, the mixture was heated at reflux for 2 h and then cooled overnight. The resulting precipitate was filtered and washed three times with EtOH/water (1:1, 10 mL). After drying under vacuum, the reaction afforded rhodamine-6G hydrazone. Yield: 0.369 g, 80%; ^{1}H NMR (400 MHz, $CDCl_3$): δ = 1.32 (t, J = 7.1 Hz, 6H), 1.92 (s, 6H), 3.22 (q, J = 6.9 Hz, 4H), 3.56 (br s, 4H), 6.26 (s, 2H), 6.39 (s, 2H), 7.06 (t, J = 3.3 Hz, 1H), 7.45 (t, J = 4.6 Hz, 2H), 7.96 ppm (t, J = 3.2 Hz, 1H); IR (neat): $\tilde{\nu}$ = 3370.6, 2921.5, 1621.4, 1516.6, 1270.3, 1203.6, 1017.8, 742.4 cm^{-1}; HRMS: m/z calcd for $C_{26}H_{28}N_4O_2$: 451.2110 $[M+Na]^+$; found: 451.2106.

Compound 1: Rhodamine hydrazone (47 mg, 0.11 mmol) was mixed with aldehyde **3** (33 mg, 0.11 mmol) in MeOH (4 mL). Glacial acetic acid (2–3 drops) was added and the mixture was stirred at RT for 4–5 h. After completion of the reaction, the precipitate was filtered and washed with MeOH until it was completely pure, as determined by TLC. Yield: 55 mg, 70%; ^{1}H NMR (400 MHz, $CDCl_3$): δ = 1.31(t, J=8 Hz, 6H), 1.86 (s, 6H), 3.19 (q, J = 4 Hz, 4H), 4.87 (s, 4H), 6.35 (d, J = 10 Hz, 4H), 6.56 (d, J = 4 Hz, 2H), 7.02–7.04 (m, 1H), 7.24 (d, J = 8 Hz, 4H), 7.34 (d, J = 9 Hz, 2H), 7.44–7.46 (m, 2H), 7.67 (t, J = 8 Hz, 2H), 7.99 (t, J = 4 Hz, 1H), 8.33 (s, 1H), 8.60 ppm (d, J = 2 Hz, 2H); ^{13}C NMR (100 MHz, [D_6]DMSO): δ = 14.1, 16.9, 37.4, 65.5, 95.8, 104.9, 117.7, 122.0, 123.3, 126.9, 127.9, 129.4, 132.2, 147.3, 151.3, 152.0, 165.1 ppm; IR (neat): $\tilde{\nu}$ = 3814.6, 2917.5, 1696.5, 1518.6, 1203.0, 1093.8, 718.0 cm^{-1}; HRMS: m/z calcd for $C_{32}H_{31}N_5O_2$: 714.3531 $[M+H]^+$; found: 714.3531.

Acknowledgements

S.B. thanks DST (J.C. Bose Fellowship) for financial support. N.D. thanks CSIR for an SRF and N.K. thanks IISc for a research associateship (RA).

[1] B. A. Leniewska, B. Godlewska-Zyłkiewicz, B. Bocca, S. Caimi, S. Caroli, A. Hulanicki, *Sci. Total Environ.* **2004**, *321*, 93.
[2] a) K. C. Nicolaou, P. G. Bulger, D. Sarlah, *Angew. Chem. Int. Ed.* **2005**, *44*, 4442; *Angew. Chem.* **2005**, *117*, 4516; b) G. Zeni, R. C. Larock, *Chem. Rev.* **2004**, *104*, 2285; c) L. F. Tietze, H. Ila, H. P. Bell, *Chem. Rev.* **2004**, *104*, 3453.
[3] S. T. Omaye, *Toxicology* **2002**, *180*, 139.
[4] R. Merget, G. Rosner, *Sci. Total Environ.* **2001**, *270*, 165.
[5] a) K. Ravindra, L. Bencs, R. Van Grieken, *Sci. Total Environ.* **2004**, *318*, 1; b) T. Liu, S. D. Lee, R. S. Bhatnagar, *Toxicol. Lett.* **1979**, *4*, 469.
[6] C. E. Garrett, K. Prasad, *Adv. Synth. Catal.* **2004**, *346*, 889.
[7] J. C. Ely, C. R. Neal, C. F. Kulpa, M. A. Schneegurt, J. A. Seidler, J. C. Jain, *Environ. Sci. Technol.* **2001**, *35*, 3816.
[8] a) F. Song, A. L. Garner, K. Koide, *J. Am. Chem. Soc.* **2007**, *129*, 12354; b) A. L. Garner, K. Koide, *Chem. Commun.* **2009**, 86; c) F. Song, E. J. Carder, C. C. Kohler, K. Koide, *Chem. Eur. J.* **2010**, *16*, 13500; d) K. Inamoto, L. D. Campbell, T. Doi, K. Koide, *Tetrahedron Lett.* **2012**, *53*, 3147; e) J. M. Williams, K. Koide, *Ind. Eng. Chem. Res.* **2013**, *52*, 8612.
[9] H. Li, J. Fan, X. Peng, *Chem. Soc. Rev.* **2013**, *42*, 7943.
[10] a) S. Sun, B. Qiao, N. Jiang, J. Wang, S. Zhang, X. Peng, *Org. Lett.* **2014**, *16*, 1132; b) S. Cai, Y. Lu, S. He, F. Wei, L. Zhao, X. Zeng, *Chem. Commun.* **2013**, *49*, 822; c) R. Balamurugan, C.-C. Chien, K.-M. Wu, Y.-H. Chiu, J.-H. Liu, *Analyst* **2013**, *138*, 1564; d) H. Li, H. Guan, X. Duan, J. Hu, G. Wang, Q. Wang, *Org. Biomol. Chem.*

2013, *11*, 1805; e) H. Li, J. Fan, M. Hu, G. Cheng, D. Zhou, T. Wu, F. Song, S. Sun, C. Duan, X. Peng, *Chem. Eur. J.* **2012**, *18*, 12242; f) B. Liu, H. Wang, T. Wang, Y. Bao, F. Du, J. Tian, Q. Li, R. Bai, *Chem. Commun.* **2012**, *48*, 2867; g) X. Chen, T. Pradhan, F. Wang, J. S. Kim, J. Yoon, *Chem. Rev.* **2012**, *112*, 1910; h) B. Liu, Y. Bao, F. Du, H. Wang, J. Tian, R. Bai, *Chem. Commun.* **2011**, *47*, 1731; i) H. Kim, K.-S. Moon, S. Shim, J. Tae, *Chem. Asian J.* **2011**, *6*, 1987; j) S. Goswami, D. Sen, N. K. Das, H.-K. Fun, C. K. Quah, *Chem. Commun.* **2011**, *47*, 9101; k) H. Li, J. Fan, J. Du, K. Guo, S. Sun, X. Liu, X. Peng, *Chem. Commun.* **2010**, *46*, 1079; l) M. Santra, S.-K. Ko, I. Shin, K. H. Ahn, *Chem. Commun.* **2010**, *46*, 3964; m) J. Du, J. Fan, X. Peng, P. Sun, J. Wang, H. Li, S. Sun, *Org. Lett.* **2010**, *12*, 476; n) H. Li, J. Fan, F. Song, H. Zhu, J. Du, S. Sun, X. Peng, *Chem. Eur. J.* **2010**, *16*, 12349; o) B. Crociani, S. Antonaroli, M. Burattini, P. Paoli, P. Rossi, *Dalton Trans.* **2010**, *39*, 3665; p) M. E. Jun, K. H. Ahn, *Org. Lett.* **2010**, *12*, 2790; q) H. Li, J. Fan, J. Wang, M. Tian, J. Du, S. Sun, P. Sun, X. Peng, *Chem. Commun.* **2009**, 5904.

[11] a) N. Kumari, N. Dey, S. Bhattacharya, *Analyst* **2014**, *139*, 2370; b) N. Kumari, N. Dey, S. Bhattacharya, *RSC Adv.* **2014**, *4*, 4230; c) N. Kumari, N. Dey, S. Jha, S. Bhattacharya, *ACS Appl. Mater. Interfaces* **2013**, *5*, 2438; d) N. Dey, S. K. Samanta, S. Bhattacharya, *ACS Appl. Mater. Interfaces* **2013**, *5*, 8394; e) N. Kumari, S. Jha, S. Bhattacharya, *Chem. Asian J.* **2012**, *7*, 2805; f) N. Kumari, S. Jha, S. Bhattacharya, *J. Org. Chem.* **2011**, *76*, 8215; g) S. Bhattacharya, S. S. Mandal, *Chem. Commun.* **1996**, 1515.

[12] Y.-K. Yang, K.-J. Yook, J. Tae, *J. Am. Chem. Soc.* **2005**, *127*, 16760.

[13] A. Dhara, A. Jana, N. Guchhait, P. Ghosh, S. K. Kar, *New J. Chem.* **2014**, *38*, 1627.

[14] N. Kumari, S. Jha, S. Bhattacharya, *Chem. Asian J.* **2014**, *9*, 830.

[15] a) S. Bhattacharya, A. Srivastava, S. Sengupta, *Tetrahedron Lett.* **2005**, *46*, 3557; b) S. Bhattacharya, S. Sengupta, *Tetrahedron Lett.* **2004**, *45*, 8733.

[16] J. Jiang, H. Jiang, W. Liu, X. Tang, X. Zhou, W. Liu, R. Liu, *Org. Lett.* **2011**, *13*, 4922.

[17] C. Liu, Y. Zhang, N. Liu, J. Qiu, *Green Chem.* **2012**, *14*, 2999.

[18] R. J. T. Houk, K. J. Wallace, H. S. Hewage, E. V. Anslyn, *Tetrahedron* **2008**, *64*, 8271.

[19] N. Kumari, S. Jha, S. K. Misra, S. Bhattacharya, *ChemPlusChem* **2014**, *79*, 1059.

[20] X.-F. Yang, X.-Q. Guo, Y.-B. Zhao, *Talanta* **2002**, *57*, 883.

Received: June 9, 2014
Revised: July 10, 2014
Published online: ■■ ■■, 0000

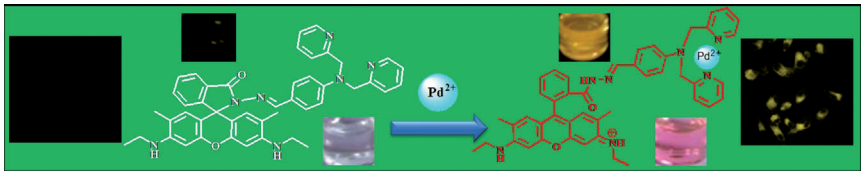

On the level: A rhodamine-based probe with a bis-picolyl binding unit has been used for the effective sub-nanomolar detection of Pd^{II} in water at physiological pH value. The probe showed instant "turn-on" response towards Pd^{II}, both in terms of color and fluorescence emission. The application of this probe has been demonstrated by detecting Pd^{II} in real water samples, pharmaceutical drugs, and cells lines.

Sensors

*Namita Kumari, Nilanjan Dey, Krishan Kumar, Santanu Bhattacharya** ____ ▮▮▮▮–▮▮▮▮

Exclusive Detection of Sub-Nanomolar Levels of Palladium(II) in Water: An Excellent Probe for Multiple Applications